Cingulate Area 32 Homologies in Mouse, Rat, Macaque and Human: Cytoarchitecture and Receptor Architecture

Brent A. Vogt,[1,2,3]* Patrick R. Hof,[4] Karl Zilles,[3,5,6] Leslie J. Vogt,[1,2] Christina Herold,[7] and Nicola Palomero-Gallagher[2,3,5]

[1]Department of Anatomy and Neurobiology, Boston University School of Medicine, Boston, Massachusetts 02118
[2]Cingulum Neurosciences Institute, Manlius, New York 13104
[3]Institute of Neuroscience and Medicine (INM-1), Research Centre Jülich, 52425 Jülich, Germany
[4]Fishberg Department of Neuroscience and Friedman Brain Institute, Ichan School of Medicine at Mount Sinai, New York, New York 10029
[5]JARA-BRAIN, Jülich-Aachen Research Alliance, 52425 Jülich, Germany
[6]Department of Psychiatry, Psychotherapy and Psychosomatics, RWTH Aachen University, 52074 Aachen, Germany
[7]C. & O. Vogt Institute of Brain Research, Heinrich-Heine-University Düsseldorf, 40225 Düsseldorf, Germany

ABSTRACT

Homologizing between human and nonhuman area 32 has been impaired since Brodmann said he could not homologize with certainty human area 32 to a specific cortical domain in other species. Human area 32 has four divisions, however, and two can be structurally homologized to nonhuman species with cytoarchitecture and receptor architecture: pregenual (p32) and subgenual (s32) in human and macaque monkey and areas d32 and v32 in rat and mouse. Cytoarchitecture showed that areas d32/p32 have a dysgranular layer IV in all species and that areas v32/s32 have large and dense neurons in layer V, whereas a layer IV is not present in area v32. Areas v32/s32 have the largest neurons in layer Va. Features unique to humans include large layer IIIc pyramids in both divisions, sparse layer Vb in area p32, and elongated neurons in layer VI, with area s32 having the largest layer Va neurons. Receptor fingerprints of both subdivisions of area 32 differed between species in size and shape, although AMPA/$GABA_A$ and NMDA/$GABA_A$ ratios were comparable among humans, monkeys, and rats and were significantly lower than in mice. Layers I–III of primate and rodent area 32 subdivisions share more similarities in their receptor densities than layers IV–VI. Monkey and human subdivisions of area 32 are more similar to each other than to rat and mouse subdivisions. In combination with intracingulate connections, the location, cytoarchitecture, and ligand binding studies demonstrate critical homologies among the four species. J. Comp. Neurol. 521:4189–4204, 2013.

INDEXING TERMS: cortex; limbic system; neurotransmitter receptors; anterior cingulate cortex; rodent; primate

Human area 32 forms the external cingulate gyrus and is bounded by the cingulate sulcus and usually the paracingulate sulcus. Although Brodmann (1909) viewed this as a homogeneous area, von Economo and Koskinas (1925) proposed that it had four subdivisions in relation to adjacent prefrontal fields referring to them (from ventral to dorsal) as FHL, FEL, FDL, and FCL. These designations correlate with our findings of four area 32 divisions; subgenual s32 is comparable to FHL, pregenual p32 to FEL and part of FDL, dorsal d32 to dorsal FDL, and midcingulate 32′ includes FCL but extends farther caudally (Vogt et al., 1995; Palomero-Gallagher et al., 2008; Vogt, 2009). The Vogts (1919) identified nine subdivisions of area 32, with three in the position of area s32, two divisions of area p32, one for area d32, and three divisions of area 32′. The s32 and p32 divisions of human anterior cingulate cortex (ACC)

Grant sponsor: James S. McDonald Foundation; Grant number: 22002078-PRH; Grant sponsor: Initiative and Networking Fund of the Helmholtz Association within the Helmholtz Alliance on Systems Biology (to K.Z.).

*CORRESPONDENCE TO: Brent A. Vogt, Department of Anatomy and Neurobiology, Boston University School of Medicine, 75 E. Concord Street, Boston, MA 02118. E-mail: bavogt@bu.edu

Received March 19, 2013; Revised May 1, 2013;
Accepted June 18, 2013.
DOI 10.1002/cne.23409
Published online July 10, 2013 in Wiley Online Library (wileyonlinelibrary.com)

are the focus of this study, because it appears that they have counterparts in murid rodent brains (Vogt and Paxinos, 2012).

Areas s32 and p32 mediate different functions and are vulnerable to different diseases. Area s32 is involved in negative (sad) emotions (Phan et al., 2002; Vogt et al., 2003). In a functional imaging study, value-dependent changes for monetary reward or physical pain activate area s32 (but not area p32) when the task requires integration of different advantages (positive values) and disadvantages (negative values) into a subjective decision (Park et al., 2011). Activation of area s32 also is proportional to the degree of confidence with which retrieval occurs (Takashima et al., 2006). In contrast, area p32 has a role in positive emotions (happiness; Phan et al., 2002; Vogt et al., 2003) and is activated during tasks requiring explicit awareness of one's emotional state (Lane et al., 1997; Piefke et al., 2003) or decisions on the affective value of sensory experiences (Grabenhorst et al., 2008; Park et al., 2011). Area p32 also has a role in memory consolidation; it links neocortical areas that store remote memory and suppress irrelevant representations (Nieuwenhuis and Takashima, 2011).

In terms of disease vulnerabilities, the following differences have been noted in the rostral divisions of area 32. Areas s32 and p32 are activated during provocation of contamination obsessions in obsessive-compulsive disorder (Saxena et al., 2009). Impairment of area p32 function occurs in schizophrenia (Preda et al., 2009), posttraumatic stress disorder (Shin et al., 2009), and apathy in probable Alzheimer's disease (Salmon and Laureys, 2009). In view of the disease vulnerabilities of areas p32 and s32, it is imperative that homologues be established between experimental animals and humans as a prelude to precise modeling of disease mechanisms.

Determining homologues between humans and nonhuman species has been impacted for more than a century by Brodmann's (1909) view that area 32 in monkeys and nonprimates could not be homologized with certainty to that in human. He emphasized this view by designating area 32 in nonhuman species "prelimbic cortex" to differentiate it from human area 32. There is overwhelming evidence that human area 32 is not homogeneous, so the issue of homologies must be revisited. Also, if area 32 in monkey and nonprimate species is "prelimbic," then, by definition, it is not part of the "limbic" cortex. Brodmann's (1909) view cannot be sustained in the context of the connections and functions of area 32; it is involved in autonomic functions (for review see Vogt and Derbyshire, 2009), projects to brainstem autonomic nuclei (Gabbott et al., 2005), and responds during and stores emotional memories (Lane et al., 1997; Phan et al., 2002; Piefke et al., 2003; Grabenhorst et al., 2008; Park et al., 2011). Thus, area 32 fits current definitions of a limbic cortex, and Brodmann's cautious statement concerning homologies between area 32 in monkey and human must be critically tested. Indeed, human areas 32′ and d32 are not present in nonhuman primates or rodents, and it is these human areas that do not have homologues in nonhuman species. The question remains of homologies of the two parts of human area 32 (p32 and s32) among the mammalian species that are frequently employed in experimental research.

A recent study of cyto- and receptor architecture of areas s32 and p32 in macaque monkey and human brains demonstrated substantial similarities, leading to the conclusion that they are homologues (Palomero-Gallagher et al., 2013). Furthermore, cytoarchitecture in mice and rats shows that area 32 comprises two parts, areas v32 and d32 (Vogt and Paxinos, 2012). This latter study, however, used Nissl-stained sections that make subtle distinctions difficult such as the dysgranular nature of layer IV, and it did not employ receptor binding analyses, which provide important quantitative information to assess area 32 subdivisions as well as establishing homologies among species. Thus, the present study seeks to extend previous rodent work (Vogt and Paxinos, 2012) with neuron-specific nuclear binding protein (NeuN) immunohistochemistry and laminar receptor binding patterns for each area in mouse, rat, macaque monkey, and human brains to evaluate homologies in the two parts of area 32 in primates (p32 and s32) and rodents (d32 and v32).

MATERIALS AND METHODS

Postmortem tissues

A human brain was obtained from the Department of Pathology at Wake Forest University School of Medicine with a postmortem interval of 3 hours and 20 minutes and a weight of 1,360 g. This is case GPC, who was an 80-year-old, right-handed, white male who died from pneumonia and a retroperitoneal hemorrhage. There was no evidence of neurological or psychiatric disorders, and the brain had an unremarkable postmortem histology. Six further human cases (ages 76 $\pm$ 3 years; four male, two female; postmortem interval 13 $\pm$ 2 hours) were obtained for receptor autoradiography through the body donor program of the Department of Anatomy, University of Düsseldorf. An adult macaque monkey was obtained at the Wake Forest University School of Medicine for immunohistochemistry, and three adult macaques were obtained from Covance

Laboratories (Münster, Germany) for receptor autoradiography. Five adult male Wistar rats (292 ± 8.6 g) and eight adult Balb mice (28.4 ± 0.79 g; five males, three females) were processed at SUNY Upstate Medical University for immunohistochemistry. Finally, eight LEW/Ztm rats were obtained from the Central Animal Facility of the Hannover Medical School and eight C57BL/6J male mice from Cerj Laboratory (Le Genest, France) and were processed for receptor autoradiography. All experimental protocols were approved by the Committee for the Humane Use of Animals at Wake Forest University School of Medicine (Winston-Salem, NC), SUNY Upstate Medical University (Syracuse, NY), and the European local committees and complied with the European Communities Council Directive.

Immunohistochemistry

The human brain was postfixed in 4% paraformaldehyde for 3 days, cryoprotected with sucrose, and sectioned on a cryostat at 50 μm thickness. The monkey was anesthetized with a lethal dose of sodium pentobarbital and intracardially perfused with 400 ml cold saline, followed by 1 liter of 4% paraformaldehyde. After 3 days of postfixation, the brain was cryoprotected in sucrose, frozen in a cryostat, and sectioned at 40 μm thickness. Mice and rats were lethally anesthetized with sodium pentobarbital and intracardially perfused with 100 ml cold saline, followed by 100–300 ml of cold 4% paraformaldehyde. After 3 days postfixation, the brains were cryoprotected in sucrose, frozen in a cryostat, and sectioned at 30 μm thickness.

The NeuN antibody (Chemicon, Temecula, CA; I.D. MAB377) is mouse monoclonal antibody AB91665 at http://antibodyregistry.org/AB 2298770. Anti-NeuN reliably detects postmitotic neurons, and Kim et al. (2009) identified it as the Fox-3 gene product with mass spectrometry of anti-NeuN immunoreactive protein, recombinant Fox-3 recognition by anti-NeuN, short hairpin RNAs targeting Fox-3 mRNA that down-regulate NeuN expression, Fox-3 expression restricted to neural tissues, anti-Fox-3 immunostaining, and complete anti-NeuN immunostaining overlapping in neuronal nuclei. The sections were pretreated with 75% methanol/25% peroxidase, followed by 3 minutes with formic acid, and then washed with distilled water and two washes in phosphate-buffered saline (PBS; pH 7.4). Sections were incubated in primary antibody in PBS (Chemicon; 1:1,000, mouse antibody) containing 0.3% Triton X-100 and 0.5 mg/ml bovine serum albumin (BSA) overnight at 4°C. After incubation in the primary antibody, the sections were rinsed in PBS and incubated in biotinylated secondary antibody at 1:200 in PBS/Triton-X/BSA for 1 hour. After rinses in PBS, sections were incubated in ABC solution (1:4; Vector Laboratories, Burlingame, CA) in PBS/Triton-X/BSA for 1 hour followed by PBS rinses and incubation in 0.05% 3.3′-diaminobenzidine and 0.01% H_2O_2 in a 1:10 dilution of PBS for 5 minutes. After final rinses in PBS, sections were mounted and counterstained with thionin.

For this comparison, we selected one case from each species, and the cytoarchitectural centroids of areas d32 and v32 in rodents and areas p32 and s32 in primates were selected for photography. The centroid was identified as the approximate center in all planes for an area and does not consider cytoarchitectural gradients that occur where two or more areas merge. These digital photographs were then entered into Photoshop CS2 and coregistered along the dorsal border of layer Va. Occasional artifacts were removed, and the contrast was enhanced in all images to reduce nonspecific neuropil staining in relation to that of individual neurons. The flat maps shown in Figure 1 were derived from previous publications for the human (Vogt, 2009), macaque monkey (Vogt et al., 2005), and rat and mouse (Vogt and Paxinos, 2012).

Receptor autoradiography

Human brains were bisected at autopsy, and each hemisphere was cut into slabs (2–3 cm thick) and frozen in isopentane at −40°C. Monkeys were killed by means of a lethal intravenous injection of sodium pentobarbital, brains immediately removed from the skull, and hemispheres frozen in isopentane at −40°C. Rats and mice were decapitated, and brains were removed from the skull and frozen in isopentane at −40°C. Unfixed frozen tissue was stored at −80°C until sectioning. Serial coronal cryosections (20 μm for human tissue, 10 μm for the other species) comprising the whole cross-section of a hemisphere were prepared using a large-scale cryostat microtome (human) or a cryostat (other species). Adjacent glass-mounted sections were processed for quantitative in vitro receptor autoradiography according to previously described protocols to label receptors for glutamate (AMPA, kainate, NMDA) and GABA ($GABA_A$, $GABA_B$, $GABA_A$-associated benzodiazepine (BZ) binding sites; Table 1; Palomero-Gallagher et al., 2008; Zilles et al., 2002), or stained with a modified silver method that produces Nissl-like images (Merker, 1983; Palomero-Gallagher et al., 2008). Binding assays consisted of a preincubation to remove endogenous ligand from the tissue, a main incubation with a tritiated ligand (total binding) or the tritiated ligand and an appropriate nonlabeled displacer (nonspecific binding), and a washing step to eliminate unbound radioactive ligand.

Radioactively labeled sections were coexposed with standards of known radioactivity concentrations against

TABLE 1.
Summary of Incubation Conditions for In Vitro Receptor Autoradiography

Receptor	[3H] ligand	Displacer	Incubation buffer	Preincubation	Main incubation	Rinsing
AMPA	AMPA (10 nM)	Quisqualate (10 μM)	50 mM Tris-acetate (pH 7.2) + 100 mM KSCN (M)[1]	3 × 10 Min at 4°C	45 Min at 4°C	4 × 4 Sec at 4°C; 2 × 2 sec fixation[2] at 4°C
Kainate	Kainate (8 nM)	Kainate (100 μM)	50 mM Tris-citrate (pH 7.1) + 10 mM Ca-acetate (M)	3 × 10 Min at 4°C	45 Min at 4°C	4 × 4 Sec at 4°C; 2 × 2 sec fixation[2] at 4°C
MDA	MK-80 (5 nM)	(+)MK-80 (100 μM)	50 mM Tris-HCl (pH7.2) + 30 μM glycine (M) + 50 μM spermidine (M)	15 Min at 22°C	60 Min at 22°C	2 × 5 Min at 4°C
$GABA_A$	Muscimol (3 nM/6 nM)[3]	GABA (10 μM)	50 mM Tris-citrate (pH 7.0)	3 × 5 Min at 4°C	40 Min at 4°C	3 × 3 Sec at 4°C
$GABA_B$	CGP 5462 (1.5 nM)	CGP 5584 (100 μM)	50 mM Tris-HCl (pH 7.2) + 2.5 mM $CaCl_2$	3 × 5 Min at 4°C	60 Min at 4°C	3 × 2 Sec at 4°C
BZ	Flumazenil (0.8 nM)	Clonazepam (2 μM)	170 mM Tris-HCl (pH 7.4)	15 Min at 4°C	60 Min at 4°C	2 × 1 Min at 4°C

[1](M): Substances added to buffer only during the main incubation.
[2]Fixation in a 100 ml/2.5 ml acetone/glutaraldehyde solution.
[3]Human and monkey sections were incubated with 3 nM of [3H]muscimol, rodents with 6 nM; BZ, $GABA_A$ associated benzodiazepine binding sites.

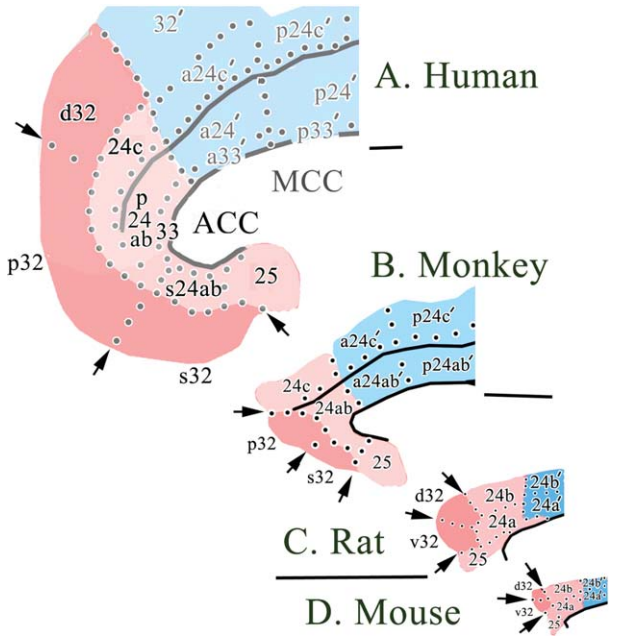

Figure 1. **A–D:** Flat maps of the medial surfaces with anterior cingulate cortex (ACC) and midcingulate cortex (MCC) color-coded for four species. The primate brains have a black line at the apex of the cingulate gyrus and one along the callosal sulcus. Arrows emphasize the areas considered in this analysis, including areas p32 and s32 for primates and areas d32 and v32 for rodents. Scale bars = 1 cm.

tritium-sensitive films for 4–18 weeks. The ensuing autoradiographs were processed densitometrically (Zilles et al., 2002). Cortical areas were anatomically identified on adjacent Nissl-stained sections, and the mean of the gray values contained in a specific area over a series of four or five sections per receptor and animal was thus transformed into a receptor concentration per unit protein (fmol/mg protein; Zilles et al. 2002). Receptor densities were extracted from linearly equidistant intensity profiles oriented vertically to the cortical surface. The area below a profile quantifies the mean areal density. Densities from layers I–III, IV and V–VI were extracted from profiles by computing the surface of discrete segments defined by the borders between layers.

Multivariate ANOVAs were applied to reveal putative, general differences in receptor densities between human and macaque monkey areas s32 and p32 as well as between rat and mouse areas d32 and v32. MANOVAs were followed by post hoc tests (paired *t*-tests) to determine which of the examined receptor types contributed to the significant difference. Multivariate ANOVAs were also applied to reveal putative, general interspecies differences in the AMPA/$GABA_A$ and NMDA/$GABA_A$ ratios for both area 32 divisions. Post

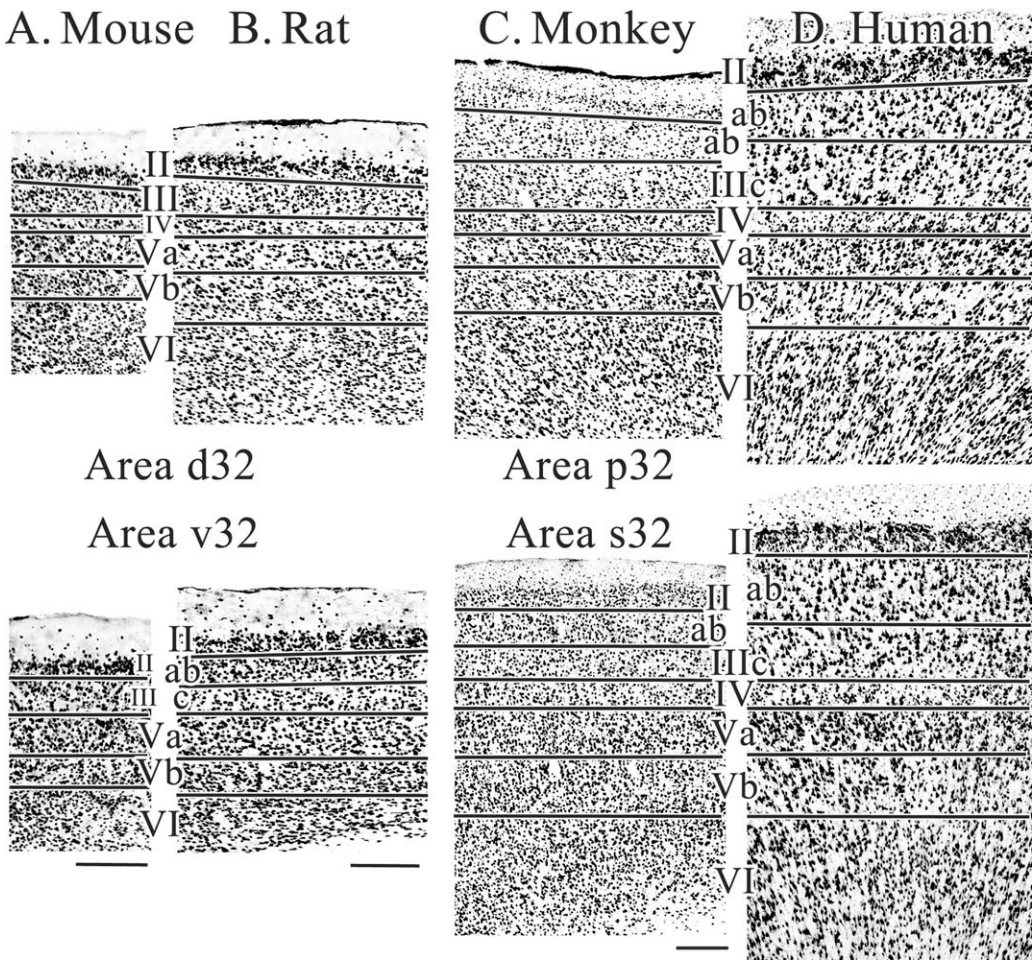

Figure 2. **A–D:** Low-magnification photographs through two area 32 divisions of four species and aligned to the top of layer Va. The key similarity in areas d32/p32 is the presence of a dysgranular layer IV. Rodent area v32 does not have a layer IV, whereas area s32 in primates does. A common feature for areas v32/s32 is the very dense layer V, with particularly large neurons. Scale bars = 250 μm.

hoc tests (*t*-tests) were then carried out to determine which species differed significantly. Significance levels for all tests were set at $P < 0.01$. Additionally, canonical (discriminant) analyses were performed with the mean areal densities or the densities extracted from layers I–III, IV, or V–VI to visualize the degree of (dis)-similarity among the four species. A hierarchical cluster analysis was conducted as previously described (Palomero-Gallagher et al., 2009) to detect putative groupings of species according to the degree of similarity of receptor architecture. Each species was represented by a matrix with four rows (two areas, each with densities extracted from superficial and deep layers) and six columns (receptors). Hierarchical clustering requires that each species be represented by a one-dimensional feature vector, so it was necessary to reduce the data. Thus, for each species, densities of a given receptor type in the set of four rows of that species were treated as a feature vector, and the Euclidean distances between all possible combinations of receptors were calculated, resulting in a new feature vector with 15 elements.

RESULTS

Cytoarchitecture

Flat maps of the divisions of ACC in Figure 1 are a schematic distillation of detailed analyses of the topography, sulcal patterns, and cytoarchitecture for the human (Vogt et al., 1995; Palomero-Gallagher et al., 2008; Vogt, 2009), macaque monkey (Vogt et al., 2005), mouse and rat (Vogt and Paxinos, 2012). Figures 2 and 3 present centroids from NeuN-immunostained sections through each part of area 32 of the four species, with the magnifications balanced slightly to enhance observation of comparative laminar similarities and differences. Figure 3 is at a higher magnification than Figure 2, showing the midcortical layers such that the structure

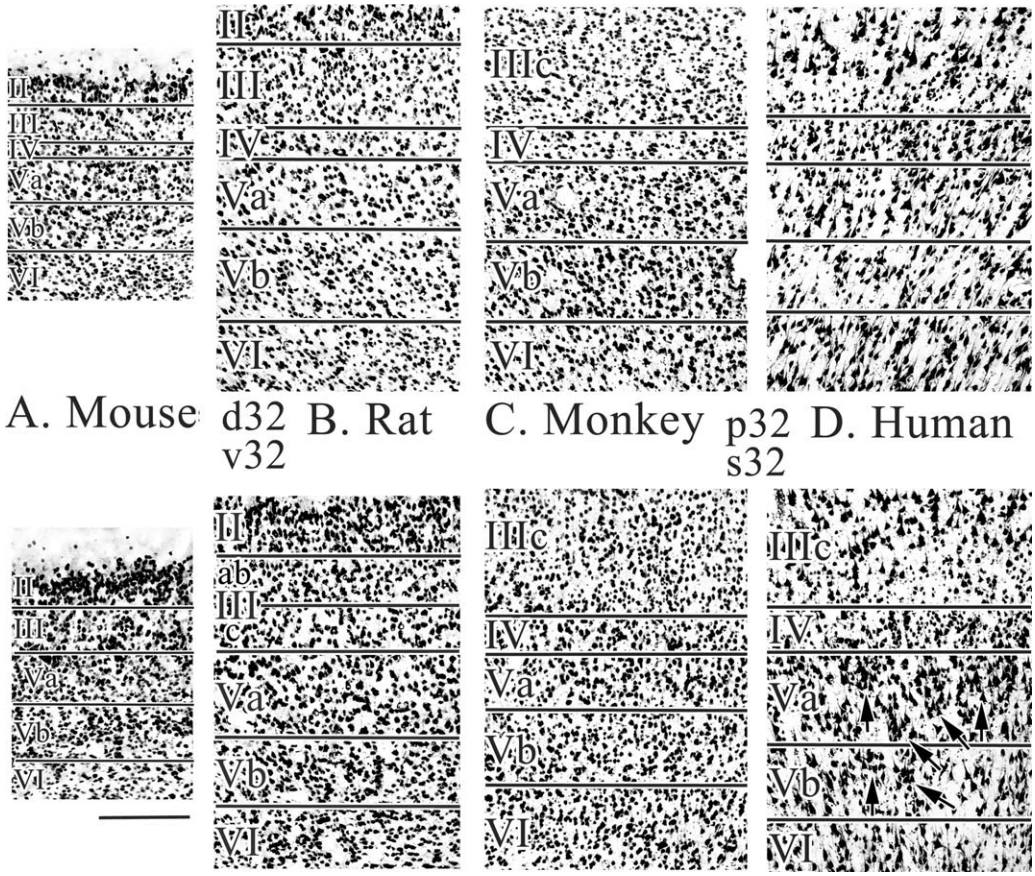

Figure 3. **A–D:** Photographs of each area 32 division through the midcortical layers at the same magnification. The sections are aligned to the top of layer Va. The arrows on human area s32 refer to clusters of neurons in layer V. Scale bar = 250 μm.

and density of neurons are more clearly appreciated. It has long been recognized that area 32 in primates has a dysgranular layer IV, and these figures also show that layer IV is present in mouse and rat area d32 but not in area v32 of either rodent. The progressive thickening of layer IV and size of neurons therein is apparent if one places mouse area d32 at one end of the spectrum and human area p32 at the other (without implying a scala naturae progression among these species). Layer III of area d32 in both rodents was not differentiated, although the rat has two divisions of layer III in area v32. Both subdivisions of area 32 in both primates had a two-part layer III. As previously noted for human (Vogt, 2009), layer IIIc neurons in area p32 are larger than those in layer IIIab, and this relationship is reversed in area s32 of both primates and the rat area v32, in which a division of layer III is notable.

Neuron densities in layers Va and Vb are particularly high in mouse area d32 and monkey area p32 and of equal densities, whereas in rat area d32 they have a higher density in layer Vb, and human area p32 densities are sparse in layer Vb. In the ventral rodent areas, layers Va and Vb both have relatively large neurons and are similarly packed, although the mouse has slightly smaller neurons in the deep part of layer Va, and packing in the rat is slightly less dense. In other words, layer V subdivisions in rodents are possible but subtle. For both primates, the relative sizes shift, with larger ones in layer Va, where neurons are also denser. Additionally, neurons in layer Va in humans form clusters (four are marked with arrows in layer Va and two in layer Vb). Similar relationships hold for layer Vb in rodents and primate areas v32 and s32, respectively, although neuron clustering appears only in the human brain. Finally, layer VI of humans is unique in both divisions of area 32, in that the neurons are generally elongated and aggregate into clusters in a cytoarchitectural feature not present in the other species (Fig. 2).

In summary, all species have a dysgranular layer IV in area d32 or p32, and areas v32 and s32 have large and dense neurons in layers Va and Vb. Features unique to rodents or primates include the following: rodent area d32 has no layer III divisions, whereas in primates there are layers IIIab and IIIc; areas v32 and

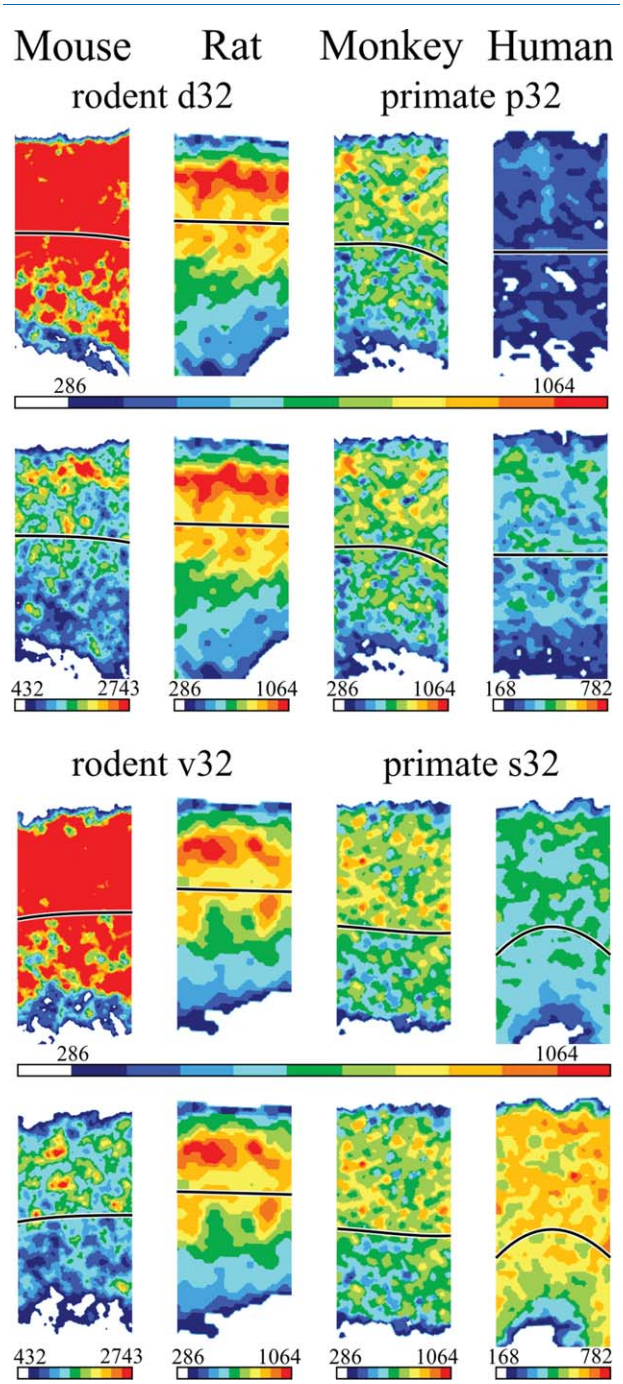

Figure 4. Color-coded autoradiographs of AMPA receptor density throughout the layers of primate areas p32 and s32 and rodent areas d32 and v32. Autoradiographs in the top row were contrast enhanced such that the scaling of absolute densities is the same for areas d32 and p32 of all species. Color-coded autoradiographs in the row below were differentially scaled to optimize the differences in receptor densities between superficial and deep layers. The different scaling is indicated by the bars, which code for densities in fmol/mg protein. Autoradiographs in the third and fourth rows show the AMPA receptor distribution in areas v32 and s32 in the same way as described above. Magnification was chosen to allow alignment of the pial surface and the layer VI/white matter border in all species, and the top of layer Va is delineated on each autoradiograph.

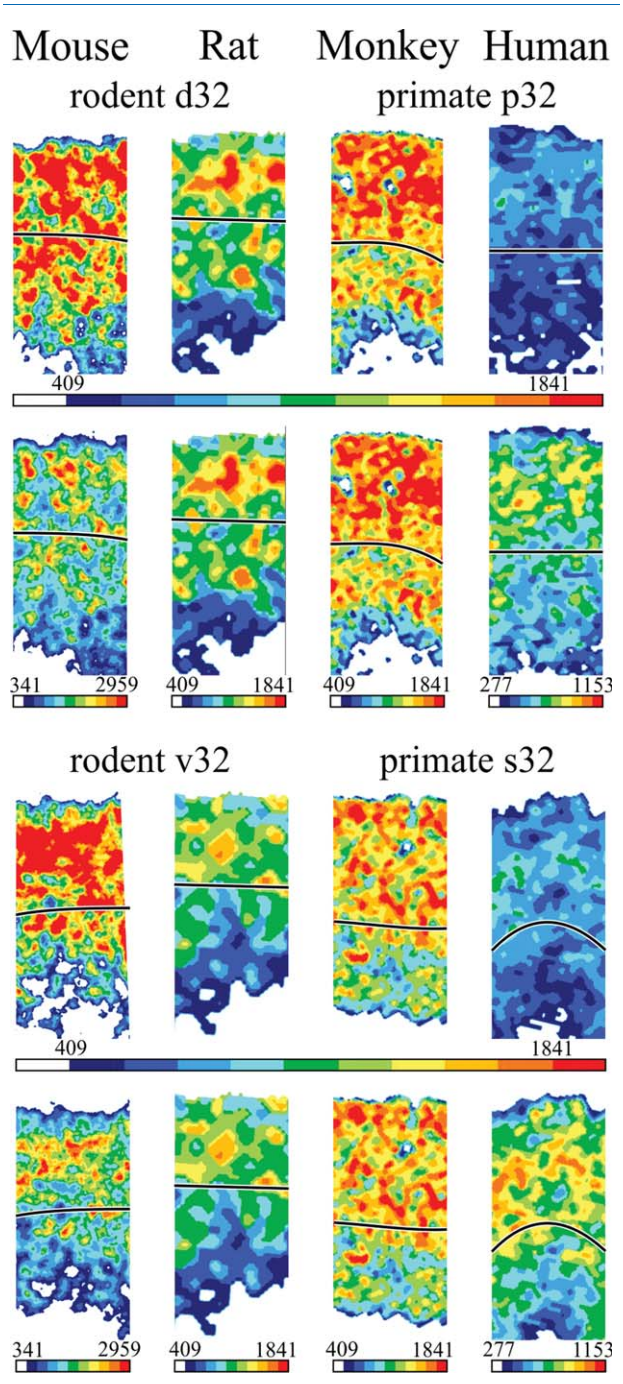

Figure 5. Color-coded autoradiographs of NMDA receptor density distribution throughout the cortical layers of primate p32 and s32 and rodent d32 and v32. For further information see Figure 4.

s32 have the relatively largest neurons in layer Va; rodent area d32 has a dysgranular layer IV, whereas area v32 in rodents does not; and area v32/s32 neuron sizes and densities are quite similar for layers Va and Vb. Features unique to human include large layer IIIc pyramids, sparse layer Vb, and elongated neurons in layer VI, and area s32 has the largest layer Va neurons that form clusters.

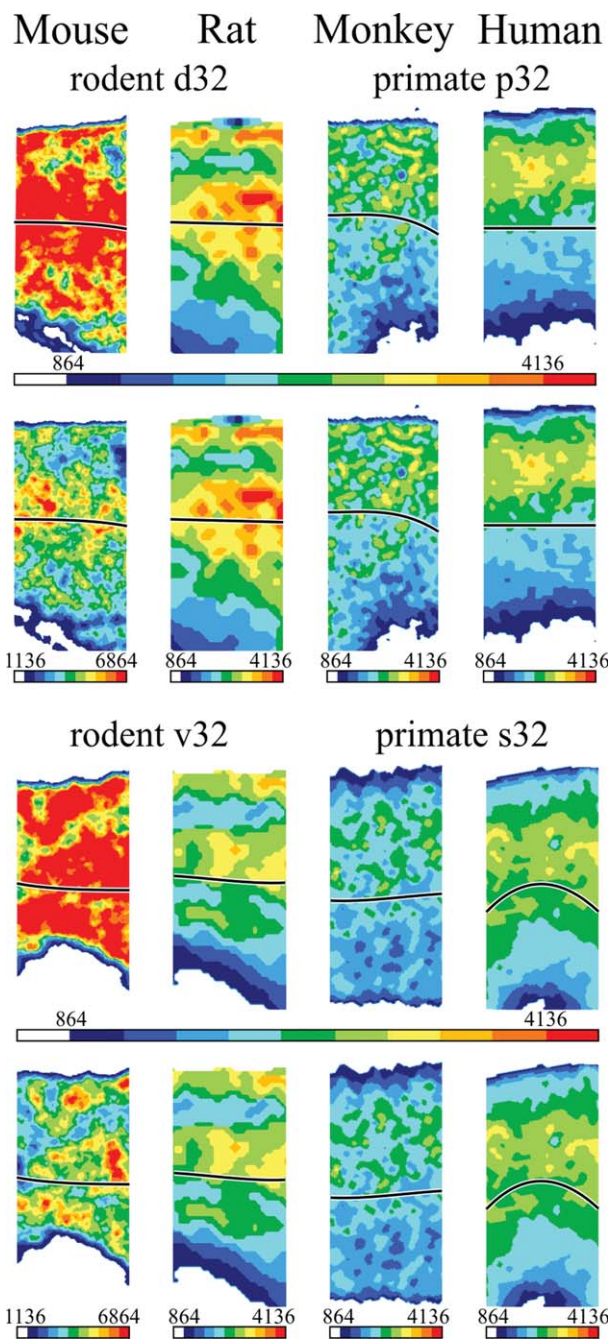

Figure 6. Color-coded autoradiographs of benzodiazepine binding site distribution throughout the cortical layers of primate p32 and s32 and rodent d32 and v32. For further information see Figure 4.

Receptor autoradiography

Six different receptor binding sites (AMPA, NMDA, kainate, $GABA_A$, $GABA_A$-associated BZ binding sites, and $GABA_B$) were studied in both subdivisions of rodent and primate area 32. As an example, the laminar distributions of AMPA, NMDA, and BZ binding sites are shown in Figures 4–6. The AMPA receptor density averaged over all cortical layers and separately for superficial and deep layers decreases with brain size (Fig. 4). In contrast to the interspecies variation in AMPA receptor densities, the NMDA receptors do not scale with brain size (Fig. 5). The NMDA receptor densities of mouse areas d32 and v32 are comparable to those of monkey areas p32 and s32, whereas rat cingulate areas have lower densities than the mouse and the human lower than the monkey (Fig. 5). The BZ binding sites of the $GABA_A$ receptor decrease in both areas d32 and v32 of rodents and p32 of monkey with brain size but increase in the superficial layers of human p32 and s32 (Fig. 6). In all species, these three receptors seem to be more densely expressed in the superficial compared with deep layers, with the notable exception of mouse area v32, where BZ binding site densities are nearly the same in superficial and deep layers.

The absolute receptor densities (fmol/mg protein) averaged over all cortical layers are depicted as receptor fingerprints in Figure 7. Here, rodent area d32 is contrasted with v32 and primate area p32 with s32. Mouse areas d32 and v32 do not differ in any of the examined receptor types (Fig. 7A). Rat areas d32 and v32 differed significantly only in their mean BZ binding site densities, which were higher in the former area (Fig. 7B). Monkey area p32 contained significantly higher NMDA but lower BZ binding site densities than did area s32 (Fig. 7C). Human areas p32 and s32 differed significantly in their AMPA, kainate, $GABA_A$, and BZ binding site densities, which were always higher in area s32 than in area p32 (Fig. 7D).

Figure 8 shows the fingerprints (fmol/mg protein) for superficial and deep layers in rodent area d32 and primate p32. Receptor densities in primate area p32 and rodent d32 tend to be more densely packed in superficial than in deep layers, with the exception of kainate receptors, which are present in higher densities in the deep layers of monkey and mouse brains (Fig. 8). However, only in mouse area d32 do kainate receptors reach significantly higher densities in the deep layers (Fig. 6A). Further significant differences between superficial and deep layers of rodent area d32 and primate p32 are demonstrated in Figure 8.

Figure 9 shows the superficial to deep layer gradients in rodent area v32 and primate s32. Again, in most cases, superficial layers show higher receptor densities than do deep layers, but only in the mouse NMDA and $GABA_A$ do receptor densities reach significant levels. Kainate receptors are more densely expressed in the deep layers and reach significance in rat area v32 and primate s32.

The search for homologies led us to evaluate the hypothesis that it is the relative proportions between excitatory and inhibitory receptors that are critical. The AMPA/$GABA_A$ and NMDA/$GABA_A$ ratios in mouse areas

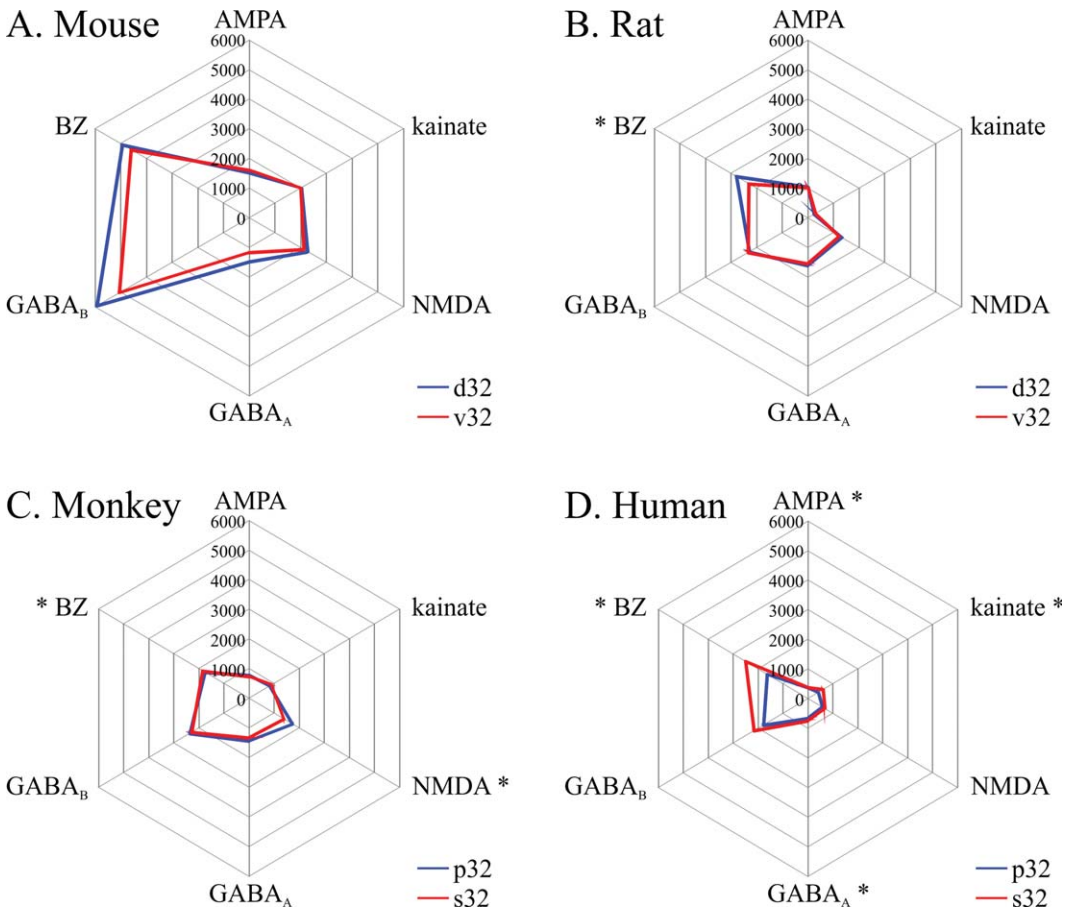

Figure 7. **A–D:** Receptor fingerprints of each area 32 subdivision. The axis codes for receptor densities in fmol/mg protein, and the same scale has been used for all plots to facilitate interspecies comparisons. Asterisks indicate significant differences ($P < 0.01$) in receptor densities between areas d32 and v32 or between areas p32 and s32; BZ, $GABA_A$-associated benzodiazepine binding sites.

d32 and v32 were significantly higher than those of their counterparts in the other three species (Fig. 10). Additionally, the NMDA/$GABA_A$ ratio in monkey area s32 was significantly higher than that of human area s32 or rat v32 (Fig. 10B).

Discriminant analyses were carried out to assess the degree of (dis)similarity of the receptor fingerprints of each area 32 division for all layers together (Fig. 11A) and separately for layers I–III (Fig. 11B), layer IV (Fig. 11C), and layers V–VI (Fig. 11D). If receptor densities are averaged over all cortical layers (Fig. 11A), it is apparent that monkey and human multireceptor fingerprints are more similar to each other than either rat or mouse, and the latter two species diverge substantially from each other. This relationship can be described by the hierarchical cluster analysis (Fig. 12), in which monkey and human contrast to rat and mouse fingerprints. The laminar discriminant analyses for the different cortical layers show the most obvious interspecies difference in layer IV, whereas layers I–III present the least interspecies divergence.

DISCUSSION

Cortical homologies among rodent areas d32/v32 and primate areas p32/s32 have been defined systematically in four ways: 1) relative location as the most rostral part of cingulate cortex in relation to landmarks (corpus callosum and callosal sulcus), rostral to midcingulate cortex (MCC), and dorsal to area 25; 2) similarities in cytoarchitecture, with a dysgranular layer IV in rodent area d32 and primate p32 and particularly large neurons in layer V of areas v32 and s32; 3) similarities of ligand binding for all receptors analyzed, with preferential binding in superficial vs. deep layers; and 4) intracingulate connection similarities, considered below.

With the present findings, we have resolved Brodmann's comparative paradox of area 32; his area 32 is not a homogeneous area but comprises areas p32/s32 in human and monkey and areas d32/v32 in rodents. The human areas d32 and 32′ have no equivalent in or homology with nonhuman primates. Although we have known this to be generally true (Vogt et al., 2005; Vogt,

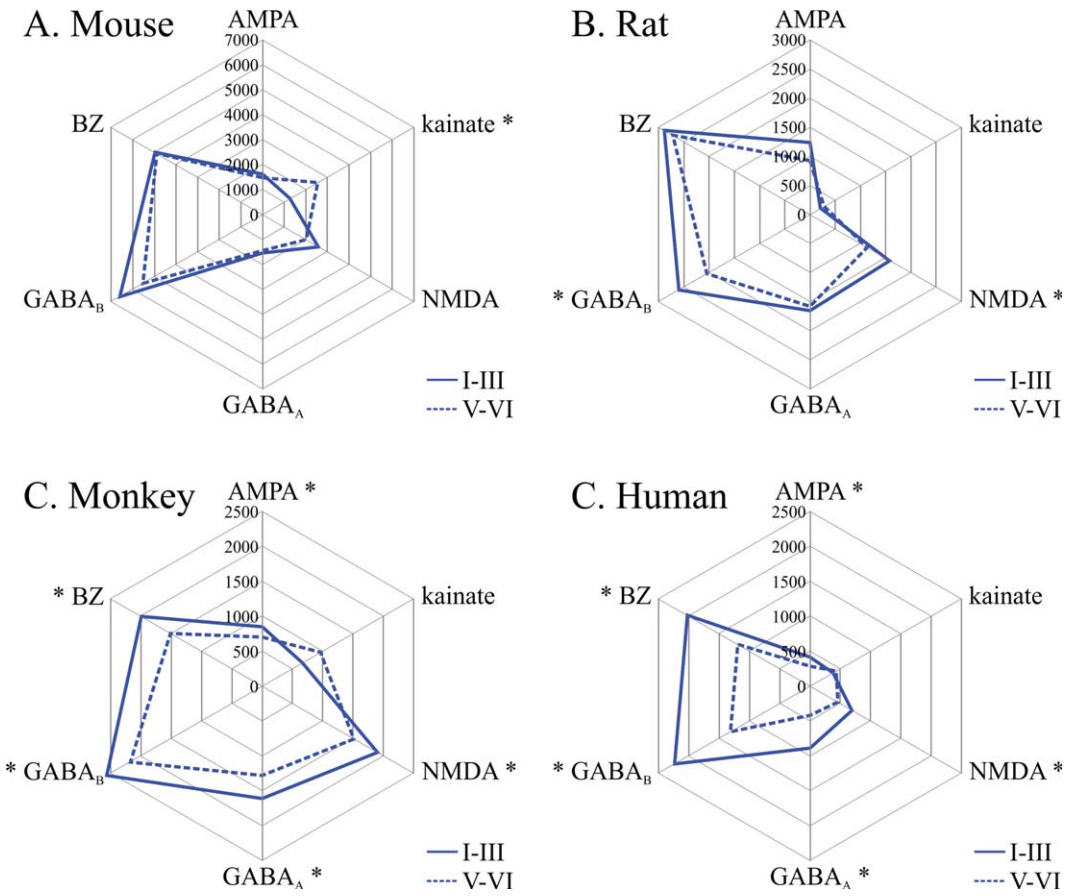

Figure 8. A–D: Receptor densities in the superficial (I–III) and deep (V–VI) layers of areas d32 (mouse and rat) and p32 (monkey and human). The axis codes for receptor densities in fmol/mg protein. Note that the scale has been set in such a way that differences in receptor densities of superficial and deep layers are displayed optimally within a given species. Asterisks indicate significant differences ($P < 0.01$) in receptor densities between superficial (I–III) and deep (V–VI) layers; BZ, $GABA_A$-associated benzodiazepine binding sites.

2009), it is now possible to state such a conclusion with more certainty in light of the exact comparisons of the other two components in mouse, rat, and macaque.

The cytoarchitecture of areas p32/d32 reflects differentiated neocortical structures, with the dysgranular layer IV progressively increasing in thickness from mouse to rat to monkey and human. Figure 3 emphasizes that neuron densities throughout midcortical layers are higher in mouse and monkey than in rat and human, and this is particularly notable in both divisions of layer V. However, human area p32 stands out in many ways from the other species; layers IIIc and V have large and dispersed pyramids generally associated with elaboration of the basal dendritic trees, and layer IV has many small neurons but also occasional clumps of larger neurons, as is characteristic of dysgranular cortex. These differences emphasize that, although each of the examined species have homologues in areas d32/p32, there are many differences as well, particularly in the human brain. The ventral and subgenual areas have significantly less laminar differentiation than the dorsal/pregenual areas and the most prominent and common feature among species is the very large and dense neurons in both parts of layer V (Fig. 3). Not all features are common; the rodents do not have a layer IV, which is present in primates, and, once again, the human has unique features, including very large pyramids in layers IIIc and V, the latter of which shows substantial clustering, and relatively more neuropil.

Densities of GABA receptors were higher than those of glutamate receptors in all species and areas, as has been reported for numerous other human and rat cortical areas (Zilles et al., 2002; Palomero-Gallagher and Zilles, 2004; Palomero-Gallagher et al., 2009; Amunts et al., 2010). Thus, the mammalian cortex appears to be subject to a strong inhibitory modulation by GABAergic neurons, and this may represent an evolutionarily conservative feature across rodents and primates. There is a trend toward higher AMPA receptor densities

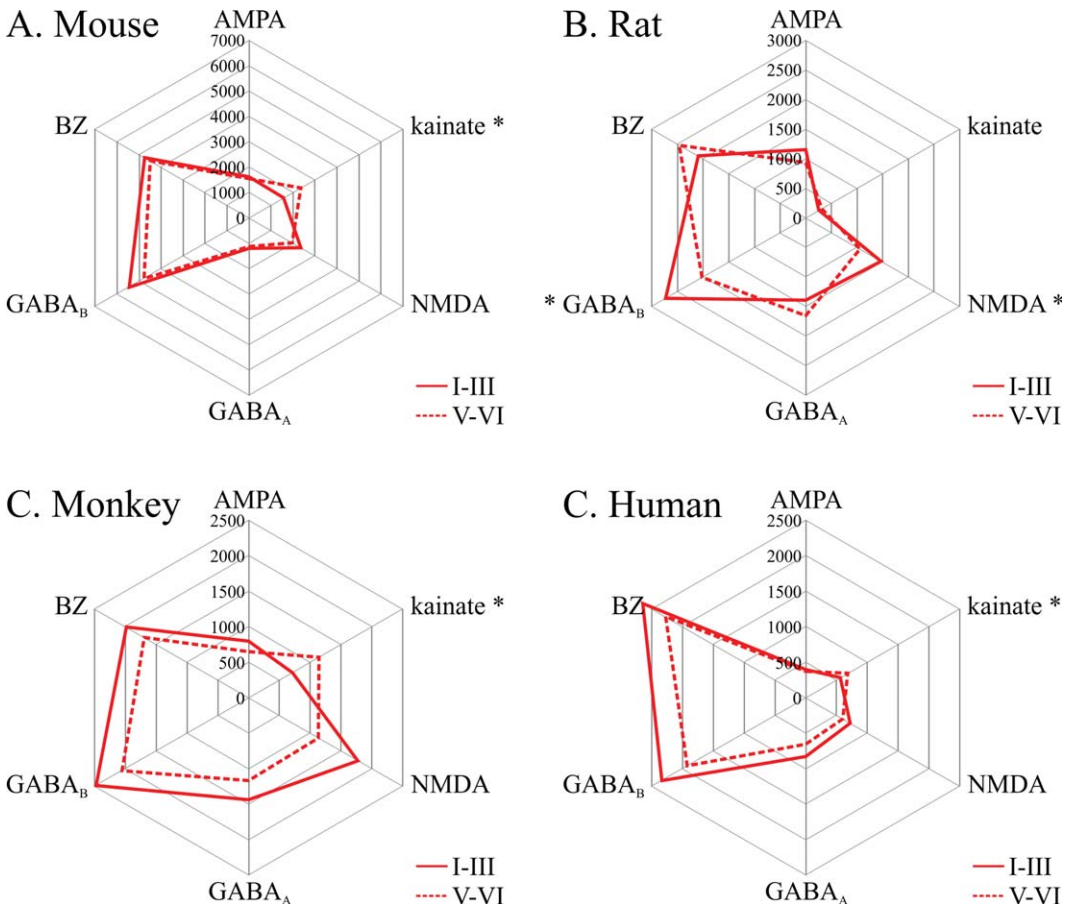

Figure 9. **A–D:** Receptor densities in the superficial (I–III) and deep (V–VI) layers of areas v32 (mouse and rat) and s32 (monkey and human). The axis codes for receptor densities in fmol/mg protein. Same scale as in Figure 5. Asterisks indicate significant differences ($P < 0.01$) in receptor densities between superficial (I–III) and deep (V–VI) layers; BZ: $GABA_A$-associated benzodiazepine binding sites.

in small brains compared with larger brains. This cannot be explained as an overproportional increase in connectivity, which would lead to more afferent and efferent fibers in all cortical layers of larger brained species, because the NMDA receptors of monkeys are more densely packed than in humans and rats, and the BZ binding sites are more densely packed in humans than in monkeys. Therefore, the differential expression of receptors between species probably reflects species-specific local differentiations in the various cortical areas and layers.

Receptor fingerprints of both subdivisions of area 32 differed between species in size and shape, supporting the notion of a species-specific pattern of multiple receptor expression, which may indicate different balances between the major excitatory and inhibitory receptors in the cingulate cortex. Indeed, AMPA/$GABA_A$ and NMDA/$GABA_A$ ratios were similar in human, monkey, and rat and differed considerably from those found in the mouse. The discriminant analyses further emphasize not only the exceptional position of receptor expression pattern in the mouse brain but also the fact that monkey and human divisions of area 32 are more similar to each other than to those of rats. Interestingly, much of the divergence among monkey, human, and rat brains disappears when binding is plotted separately for layers I–III, IV or V–VI, and this is particularly true when the discriminant analysis was carried out using only the superfical layer densities. Thus, homologies in receptor architecture are stronger in superficial than in deep layers. The examined receptors provide a substrate for homologizing human and monkey divisions of area 32 but also emphasize the differences between rodents and primates.

Most differences in receptors were found when comparing human area p32 with its counterpart in monkey, rat, and mouse brains. Human area s32 shares more similarities with monkey areas s32 and p32 than with human area p32 (Palomero-Gallagher et al., 2013). This may indicate a divergent differentiation of areas s32 and p32 between human and monkey brains at the receptor level. The cytoarchitecture of these areas in

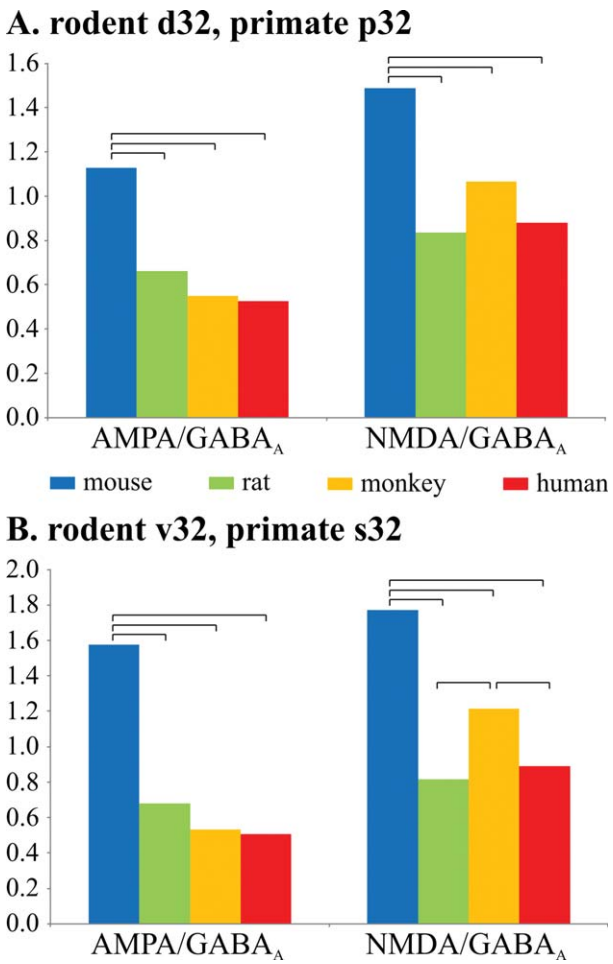

Figure 10. **A,B:** Ratios between AMPA and $GABA_A$ or NMDA and $GABA_A$ receptor densities in both area 32 divisions of human, monkey, rat, and mouse brains. Brackets indicate significant differences ($P < 0.01$).

humans and monkeys suggests the homologies indicated by the same areal designations, but further studies are necessary to understand the difference in receptor expression between human areas s32 and p32 in comparison with the monkey.

The overall pattern of cingulate cortex expansion in the four species studied here is shown in Figure 13A as a prelude to considering connections. This is a schematic drawing of each cingulate cortex based on the relative surface areas shown in Figure 1. The mouse is the smallest black oval, and surrounding ovals represent the rat, macaque, and human cingulate cortices. Each species has two parts of ACC area 32, and the arrows extend from the mouse to human brains showing this. Because the mouse and rat have but one division of MCC, this arrow stops at the monkey oval, where it splits into anterior and posterior divisions of MCC. The mouse has a retrosplenial cortex, as do all other species, so the arrow originating from the mouse retrosplenial cortex extends through all species. Finally, only the human cingulate cortex has areas d32 and 32′ (Vogt, 2009), and these are unique to humans at the apex of the cingulate expansion. The search for connection homologies must be made in the context of the extensive expansion of cingulate cortex among these species. For example, to the extent that rodents do not have areas such as dorsal and ventral posterior cingulate cortex, connections in primates cannot be assessed for these areas in rodents. The primate brain has many areas not present in rodents, including anterior cingulate area 24c, midcingulate area 24c′, a two-part MCC, and posterior cingulate areas 23 and 31.

There is one key connection similarity among these species, their intracingulate connections. Intracingulate projections of monkey area p32 terminate mainly in areas 25 and 24a–c (Pandya et al., 1981; Fig. 13B). In the rat, the connections project mainly to areas 24a,b and less to MCC areas 24a′b′ (Jones et al., 2005). The monkey retrosplenial area 30 projects to anterior cingulate area 24a but not area 32 (Morris et al., 1999), and this lack of an interaction between areas 32 and 29 is also true for the rat (van Groen and Wyss, 2003; Jones et al., 2005). In contrast, areas s32/s24a project throughout ACC and to area 23b (Vogt and Pandya, 1987; Fig. 13B). The rat and mouse do not have an area 23, so the latter connection does not exist in either species. In terms of MCC, aMCC projections in monkey terminate throughout ACC (areas p32, s32, 24, and 25; Pandya et al., 1981; Arikuni et al., 1994), whereas the one division of rat MCC projects to area 24 but not to area 32 (Jones et al., 2005). Thus, given the constraints of cytoarchitectural organization, there is a core similarity in local ACC connections of area 32 in rodents and primates.

The corticospinal system in rat is unique compared with that of the primates, in that the former originates from areas d32 and 24b and is a limbic corticospinal system. Nudo and Masterton (1990) reported a patch of retrogradely labeled neurons following cervical spinal horseradish peroxidase injections in area M2 and area 24b that is not observed in either of these areas in primates. The reason for designating this as a "limbic" system is that it directly mediates autonomic functions; i.e., a key feature of limbic areas and neurons. Area 32 projects prominently to the central autonomic area of the thoracic spinal cord, where axon terminals form asymmetric (excitatory) synapses (Bacon and Smith, 1993). This projection may also be involved in ultrasonic vocalization (Neafsey et al., 1993). Another feature that differentiates limbic corticospinal neurons is their robust innervation by the basolateral nucleus of

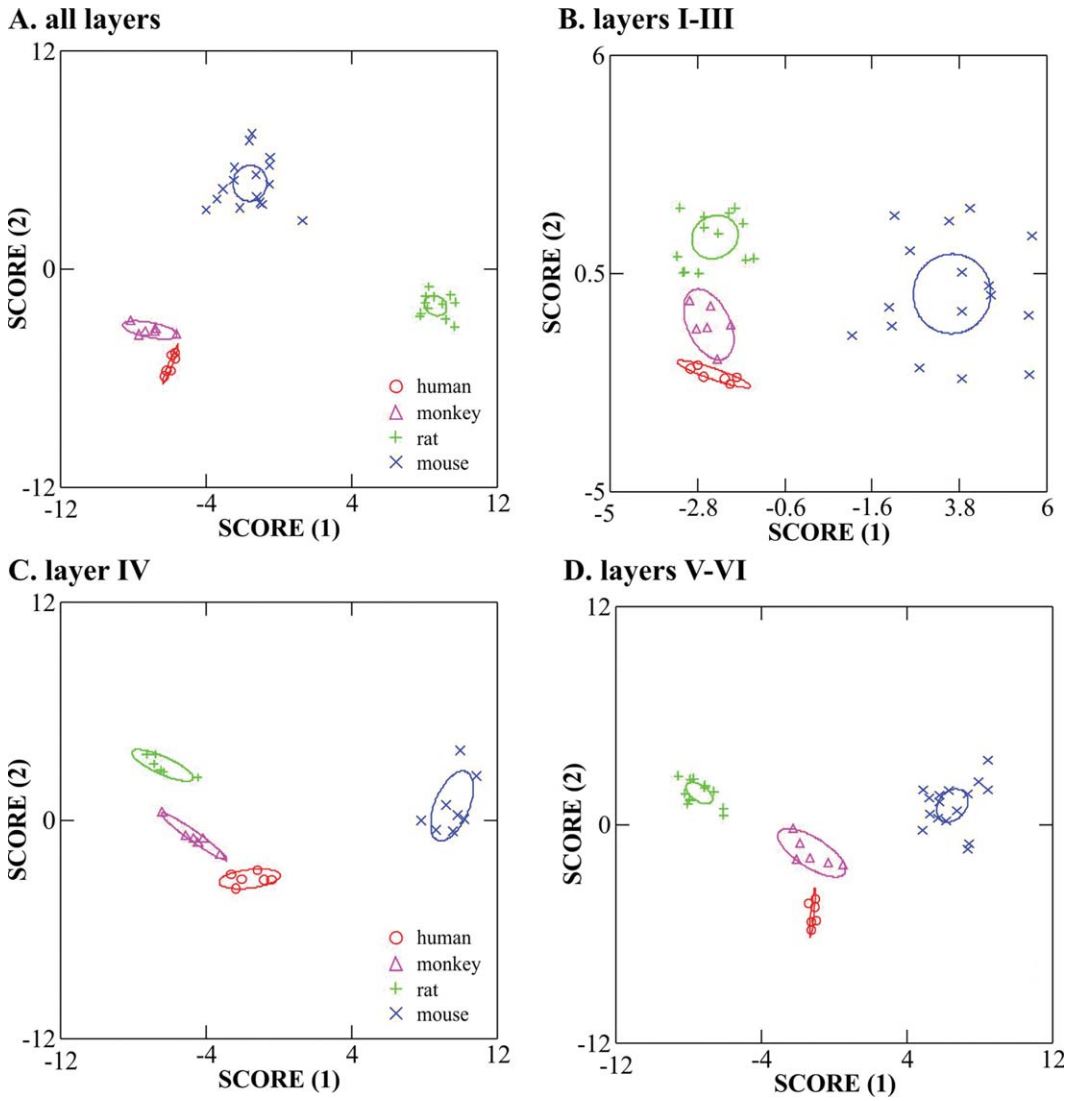

Figure 11. Plots of discriminant analyses to visualize a putative clustering of the four species based on receptor fingerprints of entire area 32 (**A**), the superficial layers (**B**), layer IV (**C**), or the deep layers (**D**). The centroids of each group are indicated by the corresponding 95% confidence intervals. Scores are the data values in a new coordinate system, with axes calculated from the original values (in this case, receptor densities) to show the differences (Euclidean distances) between the fingerprints of the four species to the greatest extent. The same scale was set for all plots. Differences are much less prominent where the superfical layers are concerned, and there is substantial overall differentiation of mouse and rat and close proximity of scores for monkey and human.

the amygdala (Vertes, 2004; Gabbott et al., 2012). Thus, the cingulospinal system in rodents mediates autonomic function and may have a small role in skeletomotor control.

The monkey area 24c on the ventral bank of the cingulate sulcus is a unique area, and it is not shared by rodents. Nevertheless, it may have a function in primates similar to that of the area d32/24b system in rodents. It is guided by auditory and visual inputs (Van Hoesen et al., 1993), it receives substantial amygdalar input (Vogt and Pandya, 1987), and it projects to the motor nucleus of the fifth nerve (Morecraft et al., 1996). It has been shown that this part of the ACC is involved in emotional vocal expressions (Müller-Preuss and Jürgens, 1976; Müller-Preuss et al., 1980). Thus, this system could have homologies to the rodent cingulospinal system in its role in emotional vocal expression. Finally, cingulate-mediated, autonomic regulation in primates is segregated from skeletomotor systems. The subgenual anterior cingulate areas s24 and s32, but not the cingulate premotor areas in the cingulate sulcus, project to autonomic brainstem structures, including the central nucleus of the amygdala, lateral hypothalamus, periaqueductal gray, and parabrachial

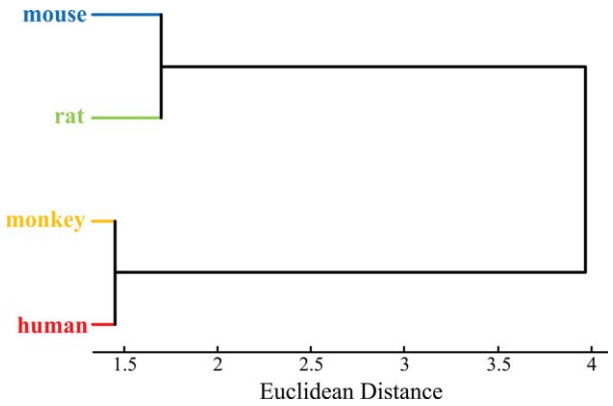

Figure 12. Hierarchical clustering of the cingulate regions of the four species examined, based on the receptor densities measured in superficial and deep layers of their area 32 divisions. Elements included in the hierarchical cluster analysis are grouped into clusters in such a way that species located in the same cluster are similar with respect to their receptor architecture and different from species in other clusters. Ward linkage algorithm; cophrenetic correlation 0.7721.

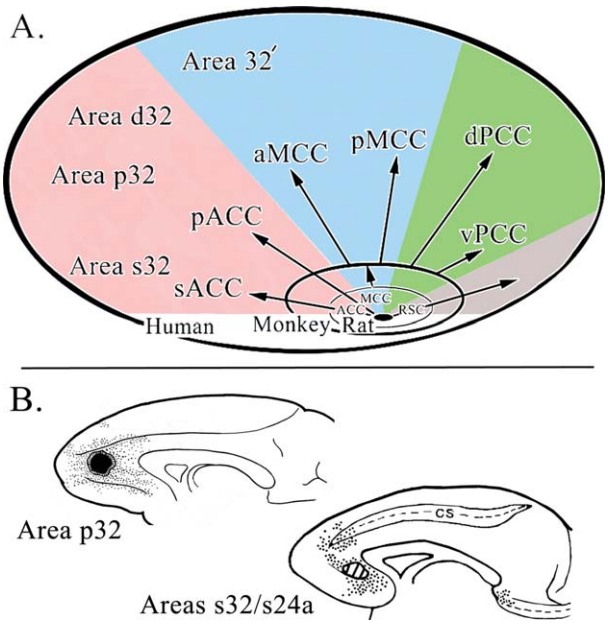

Figure 13. **A:** Differential expansion of cingulate cortex in mouse, rat, macaque, and human. The scaling for each species was derived from the proportions determined from the flat maps for the area 32 subdivisions in Figure 1. The arrows reflect the composition of each region/subregion in cingulate cortex. The ACC divisions (v32, d32, s32, and d32) appear to be homologous, and arrows are drawn through all. In contrast, the MCC has but one component in rodents, and the arrow stops at the monkey oval, where it divides into two parts and continues to the human brain for the anterior MCC (aMCC) and posterior MCC (pMCC) divisions. The human areas d32 and 32′ have no counterparts in rodents or macaque monkey and are set off as separate entities. dPCC, dorsal posterior cingulate cortex; RSC, retrosplenial cortex; vPCC, ventral posterior cingulate cortex. **B:** Intracingulate connections are shown for macaque monkey areas p32 and s32/s24a as reported by Pandya, Van Hoesen, and Mesulam (1981) and Vogt and Pandya (1987), respectively.

nucleus (Ysaui et al., 1985; Chiba et al., 2001). Thus, autonomic and skeletomotor systems are segregated in primates but not in rodents.

Homologies of cortical areas can be assessed with common ontogeny, location, structure, connections, and functions. Functional and ontogenetic homologies cannot be analyzed prior to demonstrating the location, structure, and connections of an area, and that is what has been achieved in the present studies of area 32. Areas d32 and v32 in rodents appear to be homologous to areas p32 and s32, respectively, in primates. Preuss (1995) notes that there is considerable evidence that rats possess homologues of several macaque frontal lobe areas, including the primary motor area, two divisions of premotor cortex, four divisions of cingulate cortex, and caudal orbital cortex. He also observed that rat medial frontal cortex resembles the medial frontal cortex of macaques and humans much more than the dorsolateral prefrontal cortex. This is significant in light of the evidence that the anterior cingulate cortex is involved in human diseases.

In conclusion, we have identified a number of strategies for establishing homologies among rodents and primates for two divisions of area 32. This includes the location, cytoarchitecture, laminar pattern in receptor binding, and intracingulate connections. Eventually, a multivariate model will be required to integrate the many complex factors that determine species homologues for these and other limbic cortical areas. When such models have been developed, it will be possible to search for cingulate cortex in aquatic mammals and other species that are not a routine part of experimental research but have much to offer in terms of anatomical and functional diversity.

CONFLICT OF INTEREST

The authors have no conflicts of interest to report.

ROLE OF AUTHORS

All authors had full access to all data and take responsibility for the integrity of the data and accuracy of the data analysis. Study concept and design: BAV, NP-G. Acquisition, analysis, and interpretation of the data: BAV, LJV, CH, KZ, NP-G. Drafting and critical revision of the manuscript: BAV, PRH, LJV, KZ, NP-G. Statistical analyses and illustrations: BAV, NP-G.

LITERATURE CITED

Amunts K, Lenzen M, Friederici AD, Schleicher A, Morosan P, Palomero-Gallagher N, Zilles K. 2010. Broca's region: novel organizational principles and multiple receptor mapping. PLos Biol 8.

Arikuni T, Sako H, Murata A. 1994. Ipsilateral connections of the anterior cingulate cortex with the frontal and medial temporal cortices in the macaque monkey. Neurosci Res 21:19–39.

Bacon SJ, Smith AD. 1993. A monosynaptic pathway from an identified vasomotor centre in the medial prefrontal cortex to an autonomic area in the thoracic spinal cord. Neuroscience 54:719–728.

Brodmann K. 1909. Vergleichende Lokalisationslehre der Grosshirnrinde in ihren Prinzipien dargestellt auf Grund des Zellenbaues. Leipzig: Barth.

Chiba T, Kayahara T, Nakano K. 2001. Efferent projections of infralimbic and prelimbic areas of the medial prefrontal cortex in the Japanese monkey, *Macaca fuscata*. Brain Res 888:83–101.

Gabbott PLA, Warner TA, Jays PRL, Salway P, Busby SJ. 2005. Prefrontal cortex in the rat: projections to subcortical autonomic, motor, and limbic centers. J Comp Neurol 492:145–177.

Gabbott PLA, Warner TA, Brown JB, Salway P, Gabbott T, Busby S. 2012. Amygdala afferents monosynaptically innervate corticospinal neurons in rat medial prefrontal cortex. J Comp Neurol 520:2440–2458.

Grabenhorst F, Rolls ET, Parris BA. 2008. From affective value to decision-making in the prefrontal cortex. Eur J Neurosci 28:1930–1939.

Jones BF, Groenewegen HJ, Witter MP. 2005. Intrinsic connections of the cingulate cortex in the rat suggest the existence of multiple functionally segregated networks. Neuroscience 133:193–207.

Kim KK, Adelstein RS, Kawamoto S. 2009. Identification of neuronal nuclei (NeuN) as Fox-3, a new member of the fox-1 gene family of splicing factors. J Biol Chem 284: 31052–1061.

Lane RD, Fink GR, Chau PM, Dolan RJ. 1997. Neural activation during selective attention to subjective emotional responses. Neuroreport 8:3969–3972.

Merker B. 1983. Silver staining of cell bodies by means of physical development. J Neurosci Methods 9:235–241.

Morecraft RJ, Schroeder CM, Keifer J. 1996. Organization of face representation in the cingulate cortex of the rhesus monkey. Neuroreport 7:1343–1348.

Morris R, Petrides M, Pandya DN. 1999. Architecture and connections of retrosplenial aerea 30 in the rhesus monkey (*Macaca mulatta*). Eur J Neurosci 11:2506–2518.

Müller-Preuss P, Jürgens U. 1976. Projections from the "cingular" vocalization area in the squirrel monkey. Brain Res 103:29–43.

Müller-Preuss P, Newman JD, Jürgens U. 1980. Anatomical and physiological evidence for a relationship between the "cingular" vocalization area and the auditory cortex in the squirrel monkey. Brain Res 202:307–315.

Neafsey EJ, Terreberry RR, Hurley KM, Ruitt KG, Frysztak, RJ. 1993. Anterior cingulate cortex in rodents: connections, visceral control functions, and implications for emotion. In: Vogt BA, Gabriel M, editors. Neurobiology of cingulate cortex and limbic thalamus. Boston: Birkhäuser. p 206–223.

Nieuwenhuis IL, Takashima A. 2011. The role of the ventromedial prefrontal cortex in memory consolidation. Behav Brain Res 218:325–334.

Nudo RJ, Masterton RB. 1990. Descending pathways to the spinal cord, III. Sites of origin of the corticospinal tract. J Comp Neurol 296:559–583.

Palomero-Gallagher N, Zilles K. 2004. The rat isocortex. In: Paxinos G, editor. The rat nervous system. San Diego: Academic Press. p 729–757.

Palomero-Gallagher N, Mohlberg H, Zilles K, Vogt BA. 2008. Cytology and receptor architecture of human anterior cingulate cortex. J Comp Neurol 508:906–926.

Palomero-Gallagher N, Vogt BA, Schleicher A, Mayberg HS, Zilles K. 2009. Receptor architecture of human cingulate cortex: evaluation of the four-region neurobiological model. Hum Brain Mapp 30:2336–2355.

Palomero-Gallagher N, Schleicher A, Zilles K, Vogt BA. 2013. Anterior cingulate area 32 in monkey and human: cytoarchitecture and multireceptor binding. J Comp Neurol 521:3272–3286.

Pandya DN, Van Hoesen GW, Mesulam M-M. 1981. Efferent connections of the cingulate gyrus in the rhesus monkey. Exp Brain Res 42:319–330.

Park SQ, Kahnt T, Rieskamp J, Heekeren HR. 2011. Neurobiology of value integration: when value impacts valuation. J Neurosci 31:9307–9314.

Phan KL, Wager T, Taylor SF, Liberzon I. 2002. Functional neuroanatomy of emotion: a meta-analysis of emotion activation studies in PET and fMRI. Neuroimage 16:331–348.

Piefke M, Weiss PH, Zilles K, Markowitsch HJ, Fink GR. 2003. Differential remoteness and emotional tone modulate the neural correlates of autobiographical memory. Brain 126: 650–668.

Preda A, Rilling LM, Chin RB, Tamminga CA. 2009. The cingulate gyrus in schizophrenia: Imaging and altered structure and function. In: Vogt BA, editor. Cingulate neurobiology and disease. Oxford: Oxford University Press. p 655–678.

Preuss TM. 1995. Do rats have prefrontal cortex? The Rose-Woolsey-Akert program reconsidered. J Cogn Neurosci 7: 1–24.

Salmon E, Laureys S. 2009. Brain imaging in prodromal and probable Alzheimer's disease. A focus on the cingulate gyrus. In: Vogt BA, editor. Cingulate neurobiology and disease. Oxford: Oxford University Press. p 749–762.

Saxena S, O'Neill J, Rauch SL. 2009. The role of cingulate cortex dysfunction in obsessive-compulsive disorder. In: Vogt BA, editor. Cingulate neurobiology and disease. Oxford: Oxford University Press. p 587–617.

Shin LM, Whalen PJ, Pitman RK, Rauch SL. 2009. The role of the anterior cingulate cortex in posttraumatic stress and panic disorders. In: Vogt BA, editor. Cingulate neurobiology and disease. Oxford: Oxford University Press. p 453–465.

Takashima A, Petersson KM, Rutters F, Tendolkar I, Jensen O, Zwarts MJ, McNaughton BL, Fernandez G. 2006. Declarative memory consolidation in humans: a prospective functional magnetic resonance imaging study. Proc Natl Acad Sci U S A 103:756–761.

van Groen T, Wyss JM. 2003. Connections of the retrosplenial granular b cortex in the rat. J Comp Neurol 463:249–263.

Van Hoesen GW, Morecraft RJ, Vogt BA. 1993. Connections of the monkey cingulate cortex. In: Vogt BA, Gabriel M, editors. Neurobiology of cingulate cortex and limbic thalamus. Boston: Birkhäuser. p 249–284.

Vertes RP. 2004. Differential projections of the infralimbic and prelimbic cortex in the rat. Synapse 51:32–58.

Vogt BA. 2009. Architecture, neurocytology and comparative organization of monkey and human cingulate cortices. In: Vogt BA, editor. Cingulate neurobiology and disease. Oxford: Oxford University Press. p 67–93.

Vogt BA, Derbyshire SWJ. 2009. Visceral circuits, autonomic function and human imaging. In: Vogt BA, editor.

Cingulate neurobiology and disease. Oxford: Oxford University Press. p 219–235.
Vogt BA, Palomero-Gallagher N. 2012. Cingulate cortex. In: Mai JK, Paxinos G, editors. The human nervous system, 3rd ed. Amsterdam: Academic Press. p 943–987.
Vogt BA, Pandya DN. 1987. Cingulate cortex of rhesus monkey. II. Cortical afferents. J Comp Neurol 262:271–289.
Vogt BA, Paxinos G. 2012. Cytoarchitecture of mouse and rat cingulate cortex with human homologies. Brain Struct Funct, doi 10.1007/s00429-012-0493-3.
Vogt BA, Nimchinsky EA, Vogt LJ, Hof PR. 1995. Human cingulate cortex: surface features, flat maps, and cytoarchitecture. J Comp Neurol 359:490–506.
Vogt BA, Berger GR, Derbyshire SWG. 2003. Structural and functional dichotomy of human midcingulate cortex. Eur J Neurosci 18:3134–3144.
Vogt BA, Vogt L, Farber NB, Bush G. 2005. Architecture and neurocytology of the monkey cingulate gyrus. J Comp Neurol 485:218–239.
Vogt C, Vogt O. 1919. Allegemeine Ergebnisse unserer Hirnforschung. J Psychol Neurol 25:279–462.
von Economo C, Koskinas GN. 1925. Die Cytoarchitektonik der Hirnrinde des erwachsenen Menschen. Berlin: Springer.
Yasui Y, Itoh K, Takada M, Mitani A, Kaneko T, Mizuno N. 1985. Direct cortical projections to the paraqbrachial nucleus in the cat. J Comp Neurol 234:77–86.
Zilles K, Schleicher A, Palomero-Gallagher N, Amunts K. 2002. Quantitative analysis of cyto- and receptorarchitecture of the human brain. In: Toga AW, Mazziotta JC, editors. Brain mapping. The methods. Amsterdam: Elsevier. p 573–602.